Acta Crystallographica Section D
Biological Crystallography
ISSN 0907-4449

Crystallogenesis studies on yeast aspartyl-tRNA synthetase: use of phase diagram to improve crystal quality

Claude Sauter,[a] Bernard Lorber,[a] Daniel Kern,[a] Jean Cavarelli,[b] Dino Moras[b] and Richard Giegé[a]*

[a]UPR 9002, Institut de Biologie Moléculaire et Cellulaire du CNRS, 15 rue René Descartes, F 67084 Strasbourg CEDEX, France, and [b]UPR 9004, Institut de Génétique et de Biologie Moléculaire et Cellulaire, 1 rue Laurent Fries, F 67404 Illkirch CEDEX, France

Correspondence e-mail: giege@ibmc.u-strasbg.fr

Received 29 April 1998
Accepted 14 August 1998

Aspartyl-tRNA synthetase (AspRS) extracted from yeast is heterogeneous owing to proteolysis of its positively charged N-terminus; its crystals are of poor quality. To overcome this drawback, a rational strategy was developed to grow crystals of sufficient quality for structure determination. The strategy is based on improvement of the protein homogeneity and optimization of crystallization, taking advantage of predictions from crystal-growth theories. An active mutant lacking the first 70 residues was produced and initial crystallization conditions searched. The shape and habit of initial crystals were improved by establishing a phase diagram of protein *versus* crystallizing-agent concentrations. Growth of large well faceted crystals takes place at low supersaturations near the isochronic supersolubility curve. Further refinement led to reproducible growth of two crystalline forms of bipyramidal (I) or prismatic (II) habit. Both diffract X-rays better than crystals previously obtained with native AspRS. Complete data sets were collected at 3 Å resolution for form I (space group $P4_12_12$) and form II (space group $P3_221$) and molecular-replacement solutions were found in both space groups.

1. Introduction

Purity and structural homogeneity are key parameters for optimal growth of protein crystals (Ducruix & Giegé, 1992). Chemical homogeneity improves the quality of crystals (Giegé *et al.*, 1986; Baker *et al.*, 1994; Luger *et al.*, 1997), and compact proteins like lysozyme or thaumatin, which are models for crystallogenesis studies (Rosenberger *et al.*, 1996; Ng *et al.*, 1997), have a higher propensity for crystallization than more flexible or larger multidomain proteins. Likewise, solutes stabilizing protein conformations favour crystallization (Sousa *et al.*, 1991; Jeruzalmi & Steitz, 1997). The better crystallization of proteolytic fragments or engineered protein cores compared with the whole molecules from which they derive confirms that extra domains can hinder crystallization (*e.g.* Waller *et al.*, 1971; Bergfors *et al.*, 1989; Bourguet *et al.*, 1995). Considering these stringent prerequisites, protein engineering, which provides well defined macromolecular samples (*e.g.* Barwell *et al.*, 1995), and biophysical methods such as dynamic light scattering (DLS), which verify the conformational homogeneity and crystallizability of a sample (*e.g.* Kam *et al.*, 1978; Mikol, Hirsch *et al.*, 1990; Georgalis *et al.*, 1992; Thibault *et al.*, 1992; D'Arcy *et al.*, 1993; Ferré-D'Amaré & Burley, 1997; Georgalis *et al.*, 1997), are important tools in crystallogenesis.

The multiparametric nature of crystallization and the limited knowledge of the mechanisms of nucleation and crystal growth of proteins (Ducruix & Giegé, 1992; McPherson *et al.*, 1995) have restrained most investigations to empirical

work, especially for proteins reluctant to crystallize. Statistical approaches help to explore the combinatorial diversity of crystallization conditions (Carter, 1997). However, whatever the method, the first crystals often need to be improved. Studies on model macromolecules show that phase diagrams can be useful for this purpose (Feher & Kam, 1985; Ataka & Tanaka, 1986; Chayen *et al.*, 1988; Rosenberger & Meehan, 1988; Mikol & Giegé, 1989; Riès-Kautt & Ducruix, 1992; Odahara *et al.*, 1994; Saridakis *et al.*, 1994), but they have only rarely been applied to find high-quality crystals of proteins for structure determination.

Here, we report how high-quality crystals of aspartyl-tRNA synthetase (AspRS) from yeast were obtained. For a long time, the crystals of this synthetase that could be obtained were of poor quality for structural studies because of anisotropic diffraction and low resolution (Dietrich *et al.*, 1980). It is known that this is a consequence of sequence heterogeneities. The studies reported here, which ultimately led to the growth of two crystal forms of a truncated version of yeast AspRS, were stimulated by the structural and functional information available on the $tRNA^{Asp}$ aspartylation system (Giegé *et al.*, 1996), in particular the crystallographic structures of the free tRNA (Moras *et al.*, 1980) and of its complex with AspRS (Ruff *et al.*, 1991; Cavarelli *et al.*, 1994). Crystals were obtained as the result of rational design, overexpression, purification and physicochemical characterization of a shortened but active enzyme, and the search in a crystal–solution phase diagram for crystallization conditions at low protein supersaturation. The characterization of the crystals by X-ray diffraction is presented and the theoretical background underlying their growth discussed. Practical advice on finding favourable growth conditions for protein crystals is given.

2. Materials and methods

2.1. Biochemicals and chemicals

Enzymes for DNA manipulation were from Boehringer, protease inhibitors [bestatin, pepstatin A, *trans*-epoxysuccinyl-L-leucylamido-(4-guanidino)-butane (E64)] and RNAase-free DNAase I from bovine pancreas were from Sigma, and 4-(2-aminoethyl)-benzenesulfonyl fluoride (AEBSF) was from Pentapharm (Basel). L-(^{14}C) aspartate was from Amersham, ultrapure ammonium sulfate and p*I* standards were from BDH and ultrapure sterile water was from Fresenius (Louviers). PEG 400 was from Sigma, glycerol was from Fluka, dioxan, aspartate and KSCN were from Merck, AMP-PCP was from Boehringer, octyl-β-D-glucopyranoside was from Calbiochem [repurified according to Lorber *et al.* (1990)], and Hecameg was from Vegatec (Villejuif).

2.2. AspRS-70 preparation

The original Δ70-*APS* gene, deriving from a shortened yeast *APS* gene and coding for a truncated Δ70 AspRS fused with a 14-residue-long peptide (Eriani *et al.*, 1991), was modified to eliminate the fusion peptide (Vincendon, 1990). AspRS-70, used in this work, is overexpressed in *E. coli* TGE900 cells containing the pTG908 vector that confers resistance to ampicillin (Courtney *et al.*, 1984). Its synthesis is controlled by a thermosensitive repressor, only active below 301 K and constitutively expressed by the host bacteria. Therefore, cells were first grown in enriched medium (Luria Broth made up of 12 g l^{-1} tryptone, 24 g l^{-1} yeast extract, 2.3 g l^{-1} KH_2PO_4, 16.4 g l^{-1} K_2HPO_4, 4 ml l^{-1} glycerol and 200 mg l^{-1} ampicillin) at 295 K to hinder transcription, and 2 l of a 12 h preculture was then inoculated in 25 l medium at 310 K to trigger expression. After 15 h, $\sim$800 g of cell paste was harvested and stored at 193 K.

AspRS-70 was purified in three chromatographic steps. All buffers contained 0.5 m*M* DTE and five protease inhibitors (0.1 m*M* EDTA and AEBSF; 1 μ*M* bestatin, pepstatin A and E64). Cells ($\sim$100 g), resuspended in 100 m*M* Tris–HCl pH 8.0, 10 m*M* $MgCl_2$, were sonicated and debris removed by centrifugation. The supernatant was treated by DNAase I (20 U ml^{-1}, 1 h at 277 K), dialysed in 20 m*M* potassium phosphate pH 7.2 and loaded onto a DEAE–Sephacel column (500 ml). Proteins were eluted with a 2.5 l potassium phosphate gradient (20–250 m*M*). Dialyzed active fractions were loaded on a hydroxyapatite Ultrogel column (180 ml) and eluted with a 1.8 l potassium phosphate gradient (20–300 m*M*). Active fractions were concentrated by filtration on YM30 membranes and Centricon-50 concentrators (Amicon) and buffer-exchanged against 1.5 *M* $(NH_4)_2SO_4$ with 50 m*M* Tris–HCl pH 7.4 before loading on a TSK-butyl column (300 ml) equilibrated with 2.4 *M* $(NH_4)_2SO_4$ and 50 m*M* Tris–HCl pH 7.4. This column was eluted with a 1.5 l reverse gradient from 2.4 to 0 *M* $(NH_4)_2SO_4$ in 50 m*M* Tris–HCl pH 7.4. Active fractions, concentrated to 40 mg ml^{-1} in 0.8 *M* $(NH_4)_2SO_4$ and 2 m*M* sodium cacodylate pH 6.5, were stored at 253 K.

2.3. AspRS-70 characterization

Activity assays were conducted at 310 K in 100 m*M* Na-HEPES pH 7.2, 10 m*M* ATP, 20 m*M* $MgCl_2$, 30 m*M* KCl, 0.1 m*M* L-(^{14}C) aspartate with 8 mg ml^{-1} bulk yeast tRNA, and were initiated by adding pure synthetase or cellular extracts. Note that assays are performed with subsaturated aspartate concentrations, which explains the apparently low specific activity of pure enzyme [200 U mg^{-1} instead of 2000 under saturating conditions (Lorber *et al.*, 1983)].

Protein concentration was calculated from absorbance at 280 nm ($\varepsilon_{280\,nm}$ = 0.52 ml mg^{-1} cm^{-1}). For N-terminal sequencing, proteins were blotted on ProBlott membranes (Applied Biosystems). Size-exclusion chromatography (SEC) was performed at 293 K on a Waters Protein Pak 300SW column equilibrated with 50 m*M* sodium phosphate and 100 m*M* sodium sulfate pH 6.5. Translational diffusion coefficients D_t were measured at 293 K with a dp-801 dynamic light-scattering instrument (Protein Solutions Inc., USA) on solutions containing 2 mg ml^{-1} AspRS-70 in storage buffer; hydrodynamic radii R_h were calculated using the Stokes–Einstein relation. The frictional ratio is defined as the hydrodynamic radius R_h divided by the radius of a sphere

having a partial specific volume of 0.738 $cm^3\ g^{-1}$ and the mass of the protein.

2.4. Crystallization and crystallographic methods

Crystallizations were conducted by vapour-phase diffusion using fresh protein solutions from the last purification step. Drops were prepared by mixing one volume of AspRS-70 stock with one volume of reservoir solution. The reservoir volume was 500 µl. Ammonium sulfate solutions were prepared with sterile ultrapure water and ultrapure $(NH_4)_2SO_4$, filtered over 0.22 µm membranes (Millipore) and their concentrations checked by refractometry. Before adding buffers at pH 6.8, 7.3 or 7.8, they were adjusted to the correct pH with ammonia. Sparse-matrix hanging drops were prepared from 3 µl AspRS-70 stock and 3 µl reservoir solutions (Crystal Screen, Hampton Research) at 278 K. AspRS-70 stock solution was 10 mg ml^{-1}.

The crystal-solution phase diagram was designed to explore two parameters: the concentration of ammonium sulfate in the reservoir (from 1.6 to 2.6 *M* in 0.2 *M* increments) and the initial AspRS-70 concentration in the drop (from 2.5 to 10 mg ml^{-1} in 2.5 mg ml^{-1} increments). Assays at 278 K in 16 µl sitting drops were duplicated in plates of 24 wells, one plate for observation and the second, untouched for 60 d, for solubility measurements. Optimization of the 'best' condition was performed in sitting drops of 10–20 µl. Additives were screened on a restrained concentration range of ammonium sulfate (1.9–2.1 *M* in the reservoir with 0.1 *M* increments). They included alcohols [2%(*v*/*v*) ethanol, glycerol or PEG 400], detergents (0.02 m*M* octyl-β-D-glucopyranoside or Hecameg), an organic solvent [1%(*v*/*v*) dioxan], a reducing agent (10 m*M* DTE), substrates of AspRS (1.5 m*M* aspartate, 5 m*M* ATP with 10 m*M* $MgCl_2$, 5 m*M* aspartate with 5 m*M* ATP and 10 m*M* $MgCl_2$) and a substrate analog (0.5 and 5 m*M* AMP-PCP). A broader range of ammonium sulfate concentrations (1.6–3.0 *M* with 0.1 *M* increments) was assayed for temperature and pH screening.

Solubilities were determined after 60 d, which was much longer than the time required for equilibration [1–2 d, according to Mikol, Rodeau *et al.* (1990)]. Aliquots of mother liquor were drawn from the crystallization drops, centrifuged twice (10000*g*, 10 min at 278 K to remove precipitated protein and crystals) and solubilities calculated from absorbance of the supernatant at 280 nm. Values are means with standard deviations of 10–15%.

Supersaturation is defined as $\beta = C/s$, with C the protein concentration in equilibrated drops and s the solubility. Note that another definition is $\sigma = (C - s)/C$ and an approximation is given by $\sigma = \ln\beta$ (Boistelle & Astier, 1988). Because drop volumes decrease upon vapour equilibration, final C values are higher than initial AspRS-70 concentration C_i. Since drops were prepared with AspRS-70 solutions containing 0.8 *M* ammonium sulfate, $C = C_f \times 2C_{AS}/(C_{AS} + 0.8)$, where C_{AS} is the ammonium sulfate concentration in the reservoir. Note that drops concentrate on average by a factor of 1.44 (ranging from 1.33 to 1.53) when C_{AS} rises from 1.6 to 2.6 *M*.

Complete data sets of prismatic and bipyramidal crystals were collected under cryogenic conditions (on crystals soaked for 1 min in their mother liquors containing 20% glycerol) on beamline W32 (λ = 0.97 Å, MAR Research imaging plate) at LURE (Orsay) and on beamline D2AM (λ = 1.05 Å, CCD detector) at ESRF (Grenoble), respectively. Data were reduced with the *HKL* package (Otwinowski & Minor, 1997) and processed using the *CCP*4 package (Collaborative Computational Project, Number 4, 1994).

3. Results

3.1. Design and production of a homogeneous active AspRS

The protein previously crystallized (Dietrich *et al.*, 1980) was a mixture of polypeptides starting between residues 14 and 33 (Lorber *et al.*, 1987). Its heterogeneity was responsible for poor crystal growth, and preparation of a homogeneous enzyme became a necessity. AspRS lacking the first 70 N-terminal residues (AspRS-70) was retained on the basis of previous biochemical data and structural knowledge of the AspRS–$tRNA^{Asp}$ complex. Trypsinolysis of pure AspRS showed that cleavage of the first 50–65 residues has no effect on subunit association, ATP-PPi exchange or tRNA aminoacylation (Lorber *et al.*, 1988). While enzymes starting at positions 14, 30, 50 and 70 are active, deletions beyond residue 80 lead to a loss of activity and decrease in solubility (Eriani *et al.*, 1991). Furthermore, the impossibility of assigning electron density to residues 1–67 in the map of the complex (Cavarelli *et al.*, 1994) indicated disorder in the N-terminal domain. Finally, encouragement came from preliminary assays on several AspRS deletants (Vincendon, 1990).

The absence of the lysine-rich N-terminal stretch between residues 30 and 50 in native AspRS (Lorber *et al.*, 1988) decreases the affinity of AspRS-70 for negatively charged chromatography matrices. While the entire synthetase strongly adsorbs on hydroxyapatite and is isolated pure in one step, the deletant elutes earlier and additional chromatographies are required. Protease inhibitors were present in the purification process and steps were as short as possible. Since quality was preferred over quantity, only the most active fractions were collected. About 30–40 mg (~10% yield) of pure enzyme could be obtained reproducibly from 100 g of cells.

Data on the purity and homogeneity of AspRS-70 are given in Table 1. Sequencing proved the N-terminus to be intact. DLS confirmed the homogeneity and monodispersity (within 15%) of the enzyme when stored in 0.8 *M* $(NH_4)_2SO_4$. Both DLS and SEC under native conditions gave good estimates for the molecular mass, consistent with that of the dimer (112 kDa). For AspRS purified from yeast, SEC systematically overestimated the mass, as the N-terminal extension confers an elongated shape. Compared to this protein, AspRS-70 has a smaller hydrodynamic radius and a lower frictional ratio, indicating a more globular shape. In IEF, AspRS prepared from yeast cells exhibits a large p*I* range resulting from its sequence heterogeneity, while AspRS-70 migrates as a single

Table 1
Structural properties of different forms of yeast AspRS.

Methods: A, theoretical values computed from amino-acid composition; B, SDS–PAGE; C, SEC; D, DLS; E, IEF in native conditions.

	Aspartyl-tRNA synthetase†		
	Purified from yeast‡	AspRS-70§	Method
Molecular mass M_r (kDa)			
(monomer)	59.8–61.9 (63.5†)	56.0	A
(monomer)	63 ± 5	60 ± 5	B
(dimer)	205 ± 20	120 ± 10	C
(dimer)	n.d.	111 ± 10	D
Diffusion coefficient D_t (10^{-7} cm^2 s^{-1})	n.d.	5.5 ± 0.3	D
Hydrodynamic radius R_h (nm)	n.d.	4.4 ± 0.3	D
	5.0 ± 0.5	4.6 ± 0.3	C
Frictional ratio f/f_0	1.5	1.4	C
Isoelectric point pI	5.6–7.3	5.8 ± 0.1	E

† The yeast *APS* gene encodes a polypeptide of 557 amino acids. ‡ Data from Lorber *et al.* (1983, 1987); this AspRS is a heterogeneous population of polypeptides starting at positions 14, 15, 19, 20, 21, 26, 27, 28 or 33 (see text for details). § Data are for a truncated and homogeneous protein.

population with pI 5.8. In SDS–PAGE it behaves as a polypeptide with an apparent M_r of 60 kDa (in agreement with a subunit M_r of 56 kDa). Thus, AspRS-70 is more globular and homogeneous than AspRS purified from yeast.

3.2. Optimal crystallization conditions from phase-diagram analysis

Initial crystallization conditions for AspRS-70 searched with a sparse matrix yielded crystals in an unbuffered 2.0 M $(NH_4)_2SO_4$ solution after 6 weeks. These crystals ($l < 100$ µm) exhibited growth defects and had a bipyramidal habit, similar to those obtained under different conditions with AspRS purified from yeast (Dietrich *et al.*, 1980). Several conditions with PEG as crystallizing agent led to the growth of needle-like crystals or spherulites. Note that the crystallization of AspRS-70 in ammonium sulfate is in agreement with its monodispersity in the presence of this salt, a characteristic which is a good indicator of crystallizability (Mikol, Hirsch *et al.*, 1990). It occurred with an unbuffered reservoir that dictates the pH of the drop (Mikol, Rodeau *et al.*, 1989). This pH (5.6) is close to the pI of AspRS-70 (Table 1) at which its solubility is expected to be minimal.

A two-dimensional phase diagram was established to find conditions where the crystal size is larger and the quality is improved. It is based on the above results and a broad ammonium sulfate concentration range was therefore assayed. All initial conditions were undersaturated and supersaturation was only reached after equilibration by vapour diffusion. Crystallization results were analysed after 60 d at constant temperature (278 K) and pH (5.6). Fig. 1 shows the crystallization outcomes. Three regions are identified: in the first, the synthetase remains soluble (either in an undersaturated or a metastable state); in the second, well faceted bipyramidal crystals grow at higher salt or protein concentrations; in the third, on the right-hand side of the diagram, needle-like crystals appear. From the viewpoint of the crystal grower, 'best' crystals (with well defined facets and largest size) grew reproducibly in drops with initial protein concentration C_i = 10 mg ml^{-1} equilibrated against 2.0 M $(NH_4)_2SO_4$ reservoirs (condition A3). The largest needle-like crystals grew in condition D6.

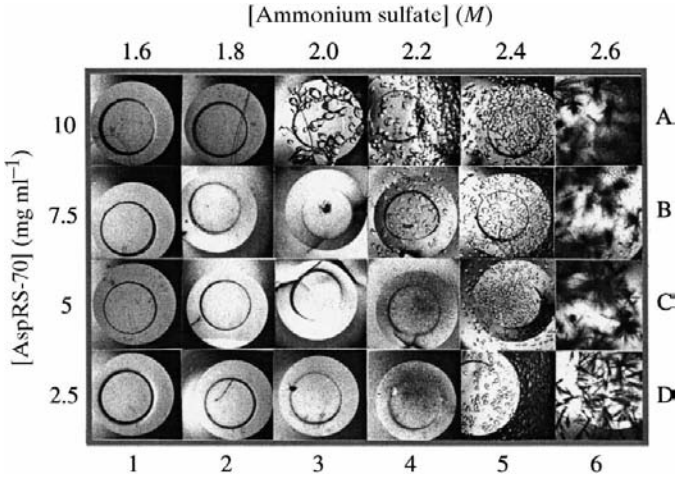

Figure 1
Two-dimensional crystal–solution phase diagram of AspRS-70 as a function of ammonium sulfate and protein concentrations. The collage displays close-up views of the centre of 24 sitting drops. Each assay is characterized by two parameters: the $(NH_4)_2SO_4$ molarity in the reservoir and the initial protein concentration in the drop. Crystallization results after 60 d at 277 K are shown at the same scale. Each view covers an area of 2.5 × 2.5 mm. The largest bipyramid (drop A3) measures ∼0.65 mm.

The solubility (s) of AspRS-70, defined as the concentrations of soluble protein remaining in equilibrium with the crystalline phase(s), was measured after 60 d. Values are plotted as a heavy line in Fig. 2. Solubility decreases from 3.8 to 1.3 mg ml^{-1} when the concentration of crystallizing agent increases from 2.0 to 2.6 M. Supersaturations calculated from solubilities by $\beta = C/s$, where C is the protein concentration in the drops after equilibration and s is the solubility, are displayed in Fig. 2 as a three-dimensional histogram. The histogram shows the isochronic supersolubility curve that separates the zone where nucleation occurs in 60 d or less from a metastable zone where AspRS-70 is not sufficiently supersaturated to nucleate in this time span. Thus, supersaturations from 2.7 to 12 are required to nucleate AspRS-70 crystals. Interestingly, at high ammonium sulfate concentrations where needles grow, small bipyramids also appear. This phenomenon, also observed with tRNA (Dock *et al.*, 1984), is explained by supersaturation changes during equilibration that favour nucleation of different crystal forms. Supersaturations needed to nucleate AspRS-70 are high when

compared with those for small molecules, but similar to those required by other proteins [*e.g.* 3–5 for porcine pancreatic α-amylase (Boistelle *et al.*, 1992) and 10 for hen egg-white lysozyme (Ataka & Asai, 1990)]. In a few drops, values could be derived for conditions where no crystals appeared after 60 d (transparent bars in Fig. 2); as anticipated they are low (from 0.9 to 3.7).

Condition A3 of the phase diagram (Figs. 1 and 2) was taken to refine further the crystallization of AspRS-70. Three series of experiments were undertaken to evaluate the effects of additives, temperature and pH in the presence of ammonium sulfate with one initial protein concentration (10 mg ml^{-1}). Additives did not have a significant effect either on the size or the number of bipyramidal crystals. Temperature screening indicated that the growth of bipyramids only occurs at 278 K. Thin needle-like crystals grow rapidly (within one day) at temperatures between 283 and 293 K and at ammonium sulfate concentrations of 2.4 *M* and above. Formation of the thin needles through a unidimensional growth process may be favoured, since there is an approximately threefold rise in the vapour-diffusion rate and drop equilibration when temperature increases from 278 to 293 K (Mikol, Rodeau *et al.*, 1990). The influence of pH was studied with buffers employed in the crystallization of free or tRNA-complexed AspRS (100 m*M* of Mes–KOH pH 6.8, Tris–maleate pH 7.3 or Tris–HCl pH 7.8) (Lorber *et al.*, 1983; Ruff *et al.*, 1988; Vincendon, 1990). Effects were dramatic: needle-like crystals observed at pH 5.6 also grew at higher pH when ammonium sulfate concentration was high (2.4 *M* and above), but a gradual increase in pH favoured three-dimensional growth. Well formed prisms grew at pH 7.8. By lowering the initial protein concentration (from 10 to 3 mg ml^{-1}) or by adding KSCN (6 m*M*), nucleation was reduced and the growth of large crystals was favoured.

To summarize, ammonium sulfate was the most favourable nucleation agent for AspRS-70. The phase diagram allowed an increase in the volume of the initial bipyramidal crystals (Fig. 3*a*, $V \simeq 8 \times 10^{-4}$ mm^3) by a factor of 40 (Fig. 3*b*, $V \simeq 3.5 \times 10^{-2}$ mm^3). Further refinement helped to define solvent conditions (at pH 7.8) for a new crystal form of prismatic habit (Fig. 3*c*), morphologically related to the tiny needle-like crystals found in the phase diagram at pH 5.6 (Fig. 1). Prismatic crystals (Fig. 3*d*) obtained at a synthetase concentration of 3 mg ml^{-1} are up to 0.8 mm long and their average volume ($V \simeq 2 \times 10^{-2}$ mm^3) is about 400 times that of the original crystals grown at the same pH with 10 mg ml^{-1} AspRS-70 (Fig. 3*c*). The size enlargement is certainly more pronounced for the needle-like crystals, but could not be quantitated accurately.

3.3. Crystallographic analyses

Crystallographic and crystallization characteristics of the two crystal forms of AspRS-70 are compared in Table 2. Bipyramids (form I) belong to tetragonal space group $P4_12_12$ (number 92) with cell parameters close to those of crystals of

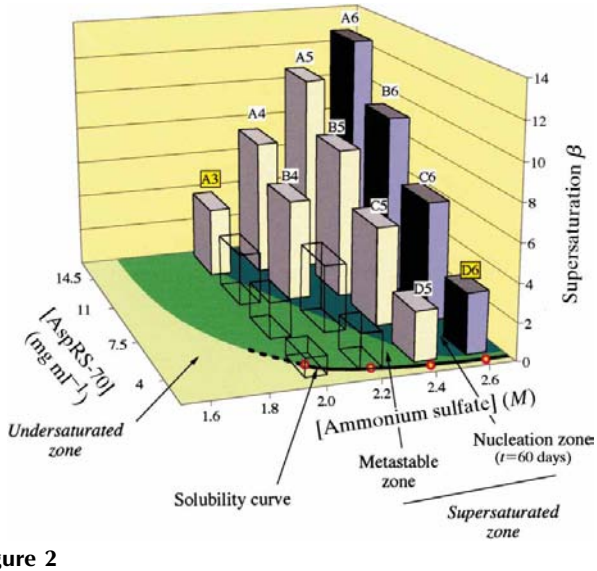

Figure 2
Experimental solubility curve and diagrammatic representation of the supersaturation in different regions of the phase diagram of AspRS-70. For each crystallization drop containing crystals (Fig. 1), solubilities were measured after 60 d and are indicated by red dots (3.8, 2.0, 1.4, 1.3 mg ml^{-1} from 2.0 to 2.6 *M* ammonium sulfate). The solubility curve is plotted as a heavy line. Undersaturated, metastable and nucleation zones are depicted in light, medium and dark green, respectively. The border between metastable and nucleation zones delineates a supersolubility curve. In the histogram, supersaturations β are depicted by transparent bars in the metastable zone and coloured bars in the nucleation zone. Light yellow bars represent conditions where bipyramidal crystals grow and purple ones where needles are predominant. The 'dead zone' corresponds to conditions D5 and D6 (see text). Conditions A3 and D6, where largest bipyramids and needle-like crystals grew, are highlighted.

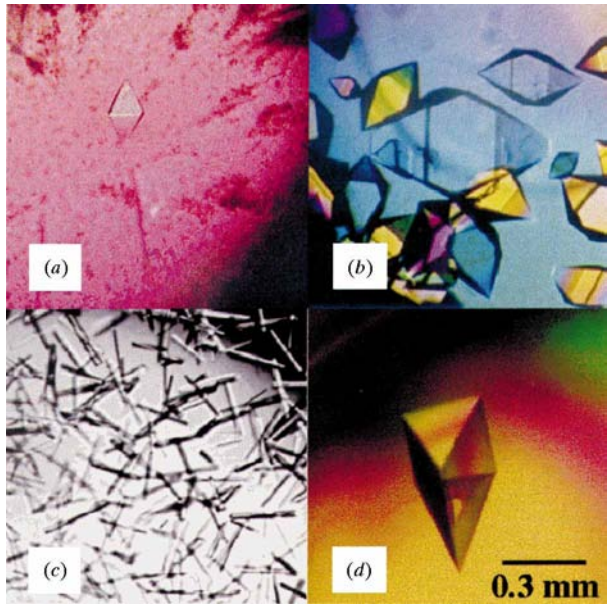

Figure 3
Increase in volume of the two crystal forms of AspRS-70 after optimization of crystallization conditions. (*a*) Best tetragonal bipyramid obtained in the sparse matrix and (*b*) crystals grown under condition A3 of the phase diagram (protein at 10 mg ml^{-1} in 2.0 *M* ammonium sulfate). (*c*) Needle-like crystals obtained at pH 7.8 and (*d*) trigonal prism after refinement (protein at 3 mg ml^{-1} in 2.6 *M* ammonium sulfate and 100 m*M* Tris–HCl at pH 7.8). All crystals are shown at the same magnification.

Table 2
Crystallization and crystallographic data of crystal forms of AspRS-70.

	Form I, bipyramids	Form II, prisms
Crystallization conditions† (278 K)		
Method	Sitting drop (20 µl)	Sitting drop (20 µl)
Protein concentration (mg ml^{-1})	14	6
Crystallizing agent	2.0 *M* $(NH_4)_2SO_4$	2.6 *M* $(NH_4)_2SO_4$
Buffer	No buffer	100 m*M* Tris–HCl
pH	5.6	7.8
Time‡	1 week	2 weeks
X-ray data collection (123 K)		
Typical crystal size (mm)	0.3 × 0.3 × 0.45	0.3 × 0.3 × 0.7
Space group§	$P4_12_12$	$P3_221$
Unit-cell parameters (Å)	$a = b = 90.8$, $c = 185.5$	$a = b = 110.7$, $c = 243.5$
Diffraction limit (Å)	≤2.7¶ (isotropic)	2.5 (anisotropic)
Completeness (%)	95 (2.95–15 Å); 88 (2.95–3.05 Å)	86 (3.0–28 Å); 85 (3.0–3.08 Å)
$R_{sym}(I)$†† and average $\langle I/\sigma(I)\rangle$	7.1%, 20 (2.95–15 Å); 9.4%, 11 (2.95–3.05 Å)	5.2%, 14 (3.0–28 Å); 8.0%, 9.3 (3.0–3.08 Å)
Molecular replacement‡‡		
Molecules in asymmetric unit	1 monomer	1 dimer
Best second-best solution	$P4_12_12$: $R = 0.44$; $C = 0.45$; $R = 0.49$, $C = 0.31$ $P4_32_12$: $R = 0.49$, $C = 0.30$; $R = 0.50$, $C = 0.29$	$P3_221$: $R = 0.46$; $C = 0.41$; $R = 0.50$, $C = 0.30$ $P3_121$: $R = 0.51$, $C = 0.25$; $R = 0.51$, $C = 0.24$

† After vapour equilibration in the drops. ‡ When first crystals appear. § See molecular-replacement data. ¶ Absolute resolution limit not determined. †† $R_{sym} = \sum_h \sum_i |\langle I_h\rangle - I_{h,i}| / \sum_h \sum_i I_{h,i}$, where $I_{h,i}$ is the intensity of a measured reflection h and $\langle I_h\rangle$ is the average intensity for this unique reflection. ‡‡ AspRS from the yeast complex (Cavarelli *et al.*, 1994) was taken as the search model. $R = \sum_h \big||F_{obs}| - |F_{calc}|\big| / \sum_h |F_{obs}|$; $C = \sum_h(|F_{obs}|^2 - \langle|F_{obs}|\rangle^2)(|F_{calc}|^2 - \langle|F_{calc}|\rangle^2) / [\sum_h(|F_{obs}|^2 - \langle|F_{obs}|\rangle^2)^2 \sum_h(|F_{calc}|^2 - \langle|F_{calc}|\rangle^2)^2]^{1/2}$.

proteolyzed AspRS ($a = b = 92$; $c = 185$ Å) grown at 6 mg ml^{-1} in 22 m*M* MES pH 6.7, 9 m*M* $MgCl_2$, 2.2 *M* $(NH_4)_2SO_4$. The latter were highly anisotropic with diffraction limits between 3.3 and 4.5 Å (Dietrich *et al.*, 1980). In contrast, the diffraction limit of AspRS-70 crystals is dramatically improved, and tetragonal crystals diffract isotropically at least to 2.7 Å. Prismatic crystals (form II), which diffract X-rays to 2.5 Å resolution with a small residual anisotropy, belong to space group $P3_121$ (number 152) or $P3_221$ (number 154). Molecular-replacement solutions were found in tetragonal and trigonal space groups using the program *AMoRe* (Navaza & Saludjian, 1997). The structure of AspRS in the complex with $tRNA^{Asp}$ (Cavarelli *et al.*, 1994) was taken as a rigid-body search model between 3 and 7 Å and good initial correlation and *R* factors were obtained (Table 2). Model building and refinement have been completed and will be published elsewhere (Sauter *et al.*, in preparation).

4. Discussion

4.1. Biochemical aspects

The rational strategy for obtaining crystals of yeast AspRS suitable for structure determination includes a thorough investigation of the biochemical and biophysical characteristics of the protein. Crystallization attempts performed on a 'crystallography grade' protein with optimum homogeneity were crucial. The design of a minimalist protein core with full enzymatic activity and control of its monodispersity at high concentration (by DLS) were pivotal. It was essential that nuclei and resulting crystals were not poisoned by impurities (defined in a broad sense). Impurities that are structurally related to the crystallizing molecule are the most harmful because they can compete during crystal formation. This was shown for the crystallizability of turkey egg-white lysozyme which is altered when contamination with hen lysozyme differing by 7 out of 129 amino acids is introduced (Abergel *et al.*, 1991). Similarly, crystallizability of hen lysozyme is altered by protein contaminants (Skouri *et al.*, 1995). The poor quality of AspRS crystals grown from chemically heterogeneous polypeptides is explained by similar effects and, indeed, it was verified that these crystals contain the proteolyzed isoforms of the synthetase (Lorber *et al.*, 1987). Noticeably, heterogeneous AspRS crystallizes better when complexed with tRNA than in the free state because complexation removes or hides heterogeneities. Crystallization bottlenecks are not peculiar to yeast AspRS. They were encoutered for *E. coli* methionyl- and asparaginyl-tRNA synthetases (Waller *et al.*, 1971; Berthet-Colominas *et al.*, 1997). The case of tryptophanyl-tRNA synthetase from *Bacillus stearothermophilus* was particularly difficult but very instructive. Genetic methods and DLS were used to improve and control its homogeneity and this synthetase became the model for the development of advanced combinatorial crystallization methods (Carter & Carter, 1979; Carter *et al.*, 1994).

4.2. Crystal-growth aspects

In the quest for better crystallizations, predictions from standard crystal-growth theories can have advantages (Mullin, 1993; Chernov, 1997) as illustrated on model proteins (McPherson *et al.*, 1995; Kurihara *et al.*, 1996; Rosenberger *et al.*, 1996). According to such theories, three-dimensional nucleation occurs at a rate increasing with supersaturation. When crystals grow, supersaturation is gradually lowered, and when it reaches that of the metastable zone, nucleation stops. At moderate supersaturation, growth mostly occurs by spiral-step propagation starting on a few dislocations; thus under these conditions growth defects are minimized. At higher supersaturation, the density of dislocations increases and growth proceeds from two-dimensional nuclei on crystal surfaces. The two mechanisms were visualized by atomic force microscopy on protein crystals (McPherson *et al.*, 1995) and it was shown that growth defects are minimized at moderate supersaturation. Techniques favouring spontaneous nuclea-

tion, like vapour diffusion, should, therefore, yield the best quality and largest crystals at the border of the nucleation zone where the number of crystals is minimal and lattice formation most regular. Lowering growth rates may improve crystal quality, but growth which is too slow, as occurs near the solubility curve in the so-called 'dead zone' (Malkin *et al.*, 1996), is known to be associated with adsorption of impurities on growing surfaces, generating defects in crystals and leading to subsequent growth cessation. From these considerations, it follows that perfection of a crystal results from a compromise and *a priori* best crystals should grow near the metastable zone at lowest supersaturation outside the 'dead zone'. As seen in Figs. 1 and 2, large AspRS-70 bipyramids grow under conditions fulfilling these criteria, namely at the highest protein concentration close to the supersolubility curve (at condition A3 rather than C5 in the 'dead zone').

In this context, the better diffracting tetragonal bipyramids of AspRS-70 are of particular interest. They belong to the same space group ($P4_12_12$) and have unit-cell parameters quasi-identical to those of the poorly diffracting crystals of native AspRS described earlier, although AspRS-70 is on average 40 amino acids shorter than the heterogeneous AspRS isolated from yeast (Table 1). Thus, isoforms of AspRS purified from yeast probably behave as competitors that introduce defects in crystals. Their deleterious effects might be enhanced under non-optimal growth conditions, as in dilute protein solutions within the 'dead zone'.

In conclusion, a few comments may be of practical use for protein crystal growers. When using spontaneous nucleation as opposed to seeding methods, crystallization should preferably proceed in the vicinity of the metastable zone, where nucleation and growth rates are moderate. However, growth conditions should be such as to minimize incorporation of impurities. Therefore, slow growth rates at low supersaturations should be avoided. Furthermore, current protein crystallization experiments imply a decrease of supersaturation during crystal growth and often last for excessively long durations. Such conditions favour growth with imperfections and poisoning. Therefore, protein crystals should be used for diffraction studies before the concentration of soluble macromolecule equals the solubility, as was performed with the AspRS-70 crystals.

We thank P. Vincendon and J.-M. Contreras for contributions at the early stages of this work. We thank also A. Théobald-Dietrich for help in protein purification, P. Dumas, G. Eriani and J. Ng for discussions, and C. Lichte and J. Reinbolt for protein sequencing. We appreciate the cooperation of M. Roth and colleagues at ESRF, R. Fourme and the team at LURE, as well as the assistance of A. Mitschler with data collection. Finally, we are indebted to A. Chernov for advice and stimulating discussions on the physics of crystal growth. This work was supported by CNRS, Ministère de la Recherche et de l'Enseignement Supérieur, CNES, ESA and Université Louis Pasteur, Strasbourg.

References

Abergel, C., Nesa, M. P. & Fontecilla-Camps, J. C. (1991). *J. Cryst. Growth*, **110**, 11–19.
Ataka, M. & Asai, M. (1990). *Biophys. J.* **58**, 807–811.
Ataka, M. & Tanaka, S. (1986). *Biopolymers*, **25**, 337–350.
Baker, H. M., Day, C. L., Norris, G. E. & Baker, E. N. (1994). *Acta Cryst.* D**50**, 380–384.
Barwell, J. A., Bochkarev, A., Pfuetznze, R. A., Tong, H., Yang, D. S. C., Frappier, L. & Edwards, A. M. (1995). *J. Biol. Chem.* **270**, 20556–20559.
Bergfors, T., Rouvinen, J., Lehtovaara, P., Caldentey, X., Tomme, P., Claeyssens, M., Pettersson, G., Knowles, T. T. & Jones, T. A. (1989). *J. Mol. Biol.* **209**, 167–169.
Berthet-Colominas, C., Seignovert, L., Cusack, S. & Leberman, R. (1997). *Acta Cryst.* D**53**, 195–196.
Boistelle, R. & Astier, J.-P. (1988). *J. Cryst. Growth*, **90**, 14–30.
Boistelle, R., Astier, J.-P., Marchis-Mouren, G., Desseaux, V. & Haser, R. (1992). *J. Cryst. Growth*, **123**, 109–120.
Bourguet, W., Ruff, M., Chambon, P., Gronemeyer, H. & Moras, D. (1995). *Nature (London)*, **375**, 377–382.
Carter, C. W. Jr (1997). *Methods Enzymol.* **276**, 74–99.
Carter, C. W. & Carter, C. W. Jr (1979). *J. Biol. Chem.* **254**, 12219–12223.
Carter, C. W. Jr, Doublié, S. & Coleman, D. E. (1994). *J. Mol. Biol.* **238**, 346–365.
Cavarelli, J., Rees, B., Eriani, G., Ruff, M., Boeglin, M., Gangloff, J., Thierry, J.-C. & Moras, D. (1994). *EMBO J.* **13**, 327–337.
Chayen, N. E., Akins, J., Campbell-Smith, S. & Blow, D. M. (1988). *J. Cryst. Growth*, **90**, 112–116.
Chernov, A. A. (1997). *Phys. Rep.* **288**, 61–75.
Collaborative Computational Project, Number 4 (1994). *Acta Cryst.* D**50**, 760–763.
Courtney, M., Buchwalder, A., Tessier, L. H., Jaye, M., Benavente, A., Balland, A., Kohli, V., Lathe, R., Toltsoshev, P. & Lecocq, J.-P. (1984). *Proc. Natl Acad. Sci. USA*, **81**, 669–673.
D'Arcy, A., Banner, D. W., Janes, W., Winkler, F. K., Loetscher, H., Schönfeld, H.-J., Zulauf, M., Gentz, R. & Lesslauer, W. (1993). *J. Mol. Biol.* **229**, 555–557.
Dietrich, A., Giegé, R., Comarmond, M.-B., Thierry, J.-C. & Moras, D. (1980). *J. Mol. Biol.* **138**, 129–135.
Dock, A.-C., Lorber, B., Moras, D., Pixa, G., Thierry, J.-C. & Giegé, R. (1984). *Biochimie*, **66**, 179–201.
Ducruix, A. & Giegé, R. (1992). Editors. *Crystallization of Nucleic Acids and Proteins: a Practical Approach.* Oxford: IRL Press, Oxford.
Eriani, G., Prevost, G., Kern, D., Vincendon, P., Dirheimer, G. & Gangloff, J. (1991). *Eur. J. Biochem.* **200**, 337–343.
Feher, G. & Kam, Z. (1985). *Methods Enzymol.* **114**, 77–111.
Ferré-D'Amaré, A. R. & Burley, S. (1997). *Methods Enzymol.* **274**, 157–166.
Georgalis, Y., Umbach, P., Raptis, J. & Saenger, W. (1997). *Acta Cryst.* D**53**, 703–712.
Georgalis, Y., Zouni, A. & Saenger, W. (1992). *J. Cryst. Growth*, **118**, 360–364.
Giegé, R., Dock, A.-C., Kern, D., Lorber, B., Thierry, J.-C. & Moras, D. (1986). *J. Cryst. Growth*, **76**, 454–561.
Giegé, R., Florentz, C., Kern, D., Gangloff, J., Eriani, G. & Moras, D. (1996). *Biochimie*, **78**, 605–623.
Jeruzalmi, D. & Steitz, T. A. (1997). *J. Mol. Biol.* **274**, 748–756.
Kam, Z., Shore, H. B. & Feher, G. (1978). *J. Mol. Biol.* **123**, 539–555.
Kurihara, K., Miyashita, S., Sazaki, G., Nakada, T., Suzuki, Y. & Komatsu, H. (1996). *J. Cryst. Growth*, **166**, 904–908.
Lorber, B., Bishop, J. B. & DeLucas, L. J. (1990). *Biochim. Biophys. Acta*, **1023**, 254–265.
Lorber, B., Kern, D., Dietrich, A., Gangloff, J., Ebel, J.-P. & Giegé, R. (1983). *Biochem. Biophys. Res. Commun.* **117**, 259–267.

Lorber, B., Kern, D., Mejdoub, H., Boulanger, Y., Reinbolt, J. & Giegé, R. (1987). *Eur. J. Biochem.* **165**, 409–417.
Lorber, B., Mejdoub, H., Reinbolt, J., Boulanger, Y. & Giegé, R. (1988). *Eur. J. Biochem.* **174**, 155–161.
Luger, K., Mader, A. W., Richmond, R. K. Sargent, D. F. & Richmond, T. J. (1997). *Nature (London)*, **389**, 251–260.
McPherson, A., Malkin, A. J. & Kuznetsov, Y. G. (1995). *Structure*, **3**, 759–768.
Malkin, A. J., Kuznetsov, Y. G. & McPherson, A. (1996). *J. Struct. Biol.* **117**, 124–137.
Mikol, V. & Giegé, R. (1989). *J. Cryst. Growth*, **97**, 324–332.
Mikol, V., Hirsch, E. & Giegé, R. (1990). *J. Mol. Biol.* **213**, 187–195.
Mikol, V., Rodeau, J.-L. & Giegé, R. (1989). *J. Appl. Cryst.* **22**, 155–161.
Mikol, V., Rodeau, J.-L. & Giegé, R. (1990). *Anal. Biochem.* **186**, 332–339.
Moras, D., Comarmond, M. B., Fischer, J., Weiss, R., Thierry, J.-C., Ebel, J.-P. & Giegé, R. (1980). *Nature (London)*, **288**, 669–674.
Mullin, J. W. (1993). *Crystallization.* Oxford: Butterworth.
Navaza, J. & Saludjian, P. (1997). *Methods Enzymol.* **276**, 581–594.
Ng, J. D., Lorber, B., Giegé, R., Koszelak, S., Day, J., Greenwood, A. & McPherson, A. (1997). *Acta Cryst.* D**53**, 724–733.
Odahara, T., Ataka, M. & Katsura, T. (1994). *Acta Cryst.* D**50**, 639–642.
Otwinowski, Z. & Minor, W. (1997). *Methods Enzymol.* **276**, 307–326.
Riès-Kautt, M. & Ducruix, A. (1992). *Crystallization of Nucleic Acids and Proteins: a Practical Approach*, edited by A. Ducruix & R. Giegé, pp. 195–218. Oxford: IRL Press.
Rosenberger, F. & Meehan, E. J. (1988). *J. Cryst. Growth*, **90**, 74–78.
Rosenberger, F., Vekilov, P. G., Muschol, M. & Thomas, B. R. (1996). *J. Cryst. Growth*, **168**, 1–27.
Ruff, M., Cavarelli, J., Mikol, V., Lorber, B., Mitschler, A., Giegé, R., Thierry, J.-C. & Moras, D. (1988). *J. Mol. Biol.* **201**, 235–236.
Ruff, M., Krishnaswamy, S., Boeglin, M., Poterszman, A., Mitschler, A., Podjarny, A., Rees, B., Thierry, J.-C. & Moras, D. (1991). *Science*, **252**, 1682–1689.
Saridakis, E. E. G., Shaw Stewart, P. D., Lloyd, L. L. & Blow, D. M. (1994). *Acta Cryst.* D**50**, 293–297.
Skouri, M., Lorber, B., Giegé, R., Munch, J.-P. & Candau, J. S. (1995). *J. Cryst. Growth*, **152**, 209–220.
Sousa, R., Lafer, E. M. & Wang, B.-C. (1991). *J. Cryst. Growth*, **110**, 237–246.
Thibault, F., Langowski, J. & Leberman, R. (1992). *J. Mol. Biol.* **225**, 185–191.
Vincendon, P. (1990). Thèse de troisième cycle, Université Louis Pasteur, Strasbourg.
Waller, J.-P., Risler, J.-L., Monteilhet, C. & Zelwer, C. (1971). *FEBS Lett.* **16**, 186–188.